Key Engineering Materials
ISSN: 1662-9795, Vol. 1056, pp 61-69
doi:10.4028/p-utjOw2

Submitted: 2025-09-12
Revised: 2026-01-09
Accepted: 2026-03-14
Online: 2026-05-20

Investigation on the Resistance Degradation of Trench SiC MOSFETs under Total Ionizing Dose Irradiation and High Drain Voltage Bias

Zhaoxu Song[a], Yu Tian[b], Zheyuan Zhang[c], Suyu Xu[d], Xiangrui Fan[e], Yiren Yu[f], Jiaxing Wei[g*], Siyang Liu[h] and Weifeng Sun[i]

The National ASIC System Engineering Research Center, School of Integrated Circuits, Southeast University, China

[a]songzhaoxu_jnu@163.com, [b]230258710@seu.edu.cn, [c]220246617@seu.edu.cn, [d]213211362@seu.edu.cn, [e]fanxiangrui@seu.edu.cn, [f]yirenyu2000@163.com, [g*]jiaxingwei@seu.edu.cn, [h]liusy2017@seu.edu.cn, [i]swffrog@seu.edu.cn

Keywords: resistance degradation, trench SiC MOSFETs, total ionizing dose (TID) effect, high drain voltage bias, positive charges accumulation.

Abstract. In this paper, the resistance degradation behaviors of double trench (DT) and asymmetric trench (AT) SiC MOSFETs under total ionizing dose (TID) effect and high drain voltage bias are investigated in detail. The output characteristics measurements before and after the irradiation indicate that the TID effect with high drain voltage bias increases the drain current, resulting in the On-state resistance degradation, whereas the high drain voltage bias seems to have no impact on the degradation. In particular, the DT SiC MOSFETs demonstrate a greater degree of degradation in comparison to the AT SiC MOSFETs under the same gate voltage. This phenomenon can be attributed to a more pronounced decline in the channel resistance. Simultaneously, the threshold voltage (V_{TH}), the drain leakage current (I_{DSS}), and the gate leakage current (I_{GSS}) are also measured, which can be concluded that the resistance degradation is attributable to the V_{TH} negative shifting induced by the positive charge accumulation in the gate oxide. Furthermore, the AT SiC MOSFETs have better irradiation tolerance owing to the P-shield asymmetric trench structure, exhibiting slight shift in the V_{TH}, the I_{DSS}, and the I_{GSS}. Finally, the TCAD simulations are utilized to successfully verify the degradation mechanism.

Introduction

As one of the most promising semiconductor devices, the silicon carbide (SiC) metal-oxide-semiconductor field-effect-transistors (MOSFETs) have been widely used in power electronic fields [1], such as the on-board charger (OBC), the photovoltaic inverter, and the motor drive owing to the merits of wide bandgap, high breakdown voltage, high thermal conductivity, and high switch speed. Meanwhile, SiC MOSFETs demonstrate considerable promise as potential candidates for aerospace applications [2]. However, in the complex space environment, the irradiation effects [3, 4, 5] often result in the degradation of the devices' electrical characteristics, and even failure, leading to a reduction in operation time of spacecraft and property loss. Among all those reliability issues, the total ionizing dose (TID) effect has garnered significant attention and increasing researches focusing on it [6, 7]. In particular, the SiC MOSFETs have to withstand the combined effect of the TID effect and the high drain bias in the Off-state [8, 9, 10]. It is imperative to explore the degradation behaviors and mechanism of the SiC MOSFETs under TID effect and high drain voltage bias.

Due to the differences in the gate process, SiC MOSFETs are equipped with two distinct gate technologies: planar [11] and trench [12]. For the latter case, the double trench (DT) type and the asymmetric trench (AT) type are two typical products, which both eliminate the junction field effect transistor (JFET) region, thus possessing a higher power density and a lower On-state resistance. However, there are many reports claiming that the trench SiC MOSFETs are more susceptible to the TID effect [13, 14]. For instance, Z. Fu *et al*. discovered that the AT SiC MOSFETs exhibited a more pronounced negative shifting trend in the threshold voltage (V_{TH}) compared to the planar SiC MOSFETs under the TID irradiation. R. Luo *et al*. calculated the reduction percentage of the On-state resistance (R_{DSON}) and revealed that the DT SiC MOSFETs have a higher resistance degradation rate.

J. Jiang *et al*. compared the electrical parameters degradation behaviors and the annealing responses of various devices, discovering that the TID effect exerts a profound influence on the trench structure. Indeed, the R_{DSON} is of considerable importance for the SiC MOSFETs among the literatures above, which has a strong relation with the current variations and irradiation tolerance capability. As a result, it is necessary to undertake a comprehensive evaluation of the resistance degradation and elucidate the mechanisms of the trench SiC MOSFETs under the TID irradiation with high drain bias condition.

In this work, the DT and the AT SiC MOSFETs are exposed to gamma ray irradiation with different drain biases to investigate the resistance degradation mechanism in detail. Firstly, the output characteristics at varying gate voltages are measured and the values of the main resistance components are calculated based on the measurements. It is evident that the DT SiC MOSFETs are profoundly affected by the TID effect owing to the severe degradation of the channel resistance. Subsequently, the V_{TH}, the drain leakage current (I_{DSS}), and the gate leakage current (I_{GSS}) are measured. Their results demonstrate that the resistance degradation is induced by the positive charge accumulation, which is a consequence of gamma ray exposure. Furthermore, it has been demonstrated that the P-shield structure enhances the irradiation tolerance of AT SiC MOSFETs, which is attributable to the low level of the leakage current. Finally, the TCAD simulations have been employed to successfully verify the degradation mechanism.

Experiment Conditions

In this experiment, commercial 160mΩ DT and 140mΩ AT SiC MOSFETs with the breakdown voltage over 1200V are selected as the samples and they are TO-247-3 packaged. Fig. 1 shows the schematic cross sections of the DT and the AT structure. Moreover, the Cobalt-60 (Co^{60}) gamma-ray at a dose rate of 100 rad(Si)/s is adopted as the irradiation source. The irradiation dose is set to 600krad(Si) to imitate the devices' operating situation over years in the space environment considering that the dose rate is about 0.01 rad(Si)/s near the Earth orbit. The detailed irradiation and bias conditions for the samples are listed in Table 1. Three samples are selected for each group during the irradiation so that possible deviations among devices could be minimized and hence we can obtain a credible result. Prior to the gamma ray irradiation, the electrical parameters (V_{TH}, I_{DSS}, I_{GSS}) are measured, and the post-irradiation measurements are also completed within 24 hours. The device parameters for simulations are given in Table 2.

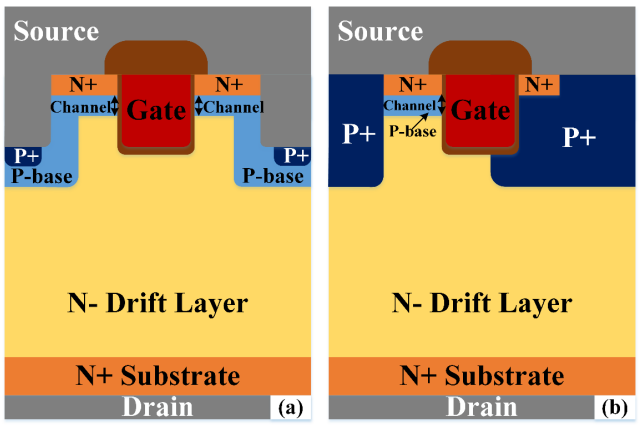

Fig. 1. Schematic cross section of (a) the DT, and (b) the AT SiC MOSFET.

Table 1. Irradiation and Drain Voltage Bias Conditions.

Type	TID(krad(Si))	Drain Voltage Bias (V)		
		600	800	1000
DT	600	Sample A1	Sample B1	Sample C1
AT	600	Sample A2	Sample B2	Sample C2

Table 2. Device Parameters for the Simulation.

Symbol	Device Parameter	Value	
		DT	AT
L_{CH}	Length of channel	0.34 μm	0.34 μm
W_{CELL}	Width of Cell	3.6 μm	2.7 μm
W_{N+}	Width of N+	0.76 μm	0.5 μm
W_{P+}	Width of P+	0.2 μm	0.5μm(left)/1.3μm(right)
$W_{P\text{-}base}$	Width of P-base	1.26 μm	0.5 μm
W_{Gate}	Width of Gate	1 μm	0.6 μm
W_{OHM}	Width of Ohm Contact	0.9 μm	0.8 μm
$T_{S\text{-}Oxide}$	Thickness of Side Oxide	50 nm	50 nm
$T_{B\text{-}Oxide}$	Thickness of Bottom Oxide	150 nm	150 nm
D_{P+}	Depth of P+	0.3 μm	1.5 μm
$D_{P\text{-}base}$	Depth of P-base	1.3 μm	0.34 μm

Results and Discussions

In this part, the electrical characteristics are measured in order to calculate the values of resistance variations and to further obtain the degradation mechanism. Meanwhile, TCAD simulations are used to validate the degradation behaviors with these measurements. As illustrated in Fig. 2, the output characteristics results of the DT and AT samples are presented. It is observed that the gamma ray irradiation leads to an augmentation in the drain current (I_{DS}), especially for the DT samples, exhibiting a more severe degradation trend. Concurrently, the drain voltage bias exerts no impact on the I_{DS}. Notably, when the gate source voltage (V_{GS}) is 12V, the I_{DS} has a drastic increase for the samples A1, B1, and C1, while it has a slight increase for the samples A2, B2, and C2. Apparently, the TID effect degrades these samples' R_{DSON}, but the degree of degradation is different.

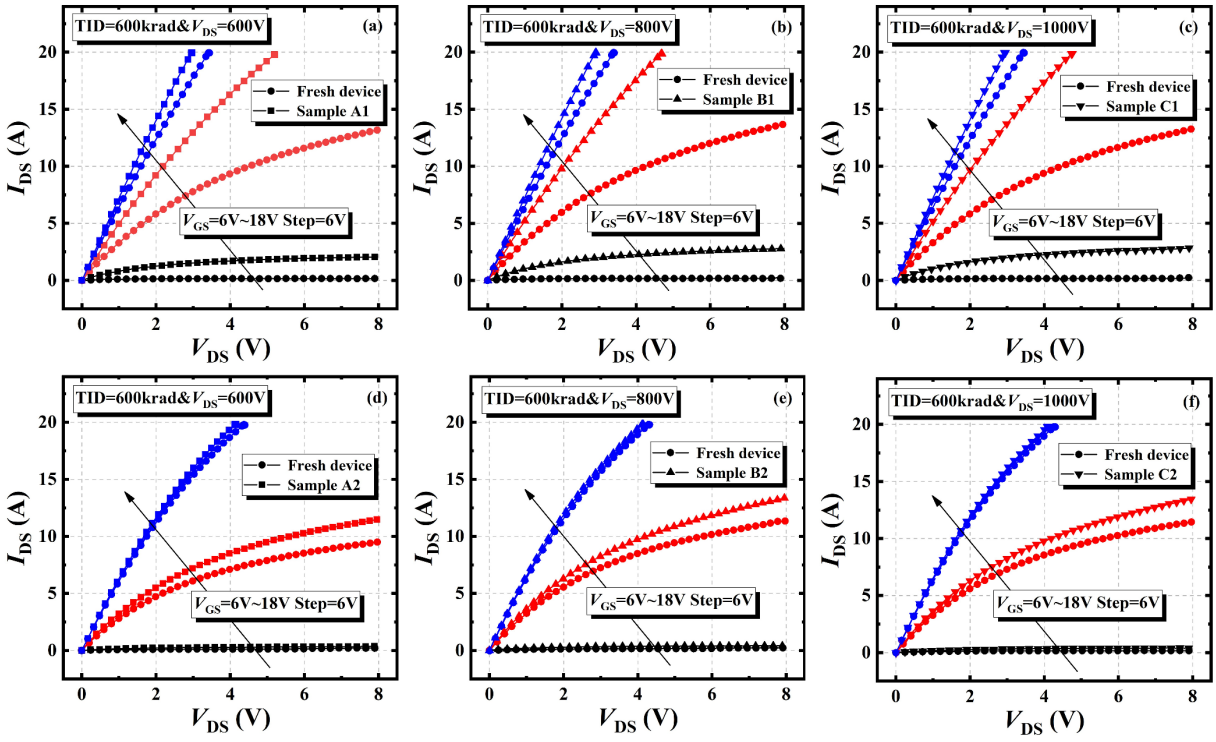

Fig. 2. Output characteristics results of the DT samples at (a) V_{DS}=600V, (b) V_{DS}=800V, (c) V_{DS}=1000V, and the AT samples at (d) V_{DS}=600V, (e) V_{DS}=800V, (f) V_{DS}=1000V with 600 krad(Si) irradiation.

In order to compare the R_{DSON} degradation behaviors between the DT samples and the AT samples, the On state resistance variations (ΔR_{DSON}) are calculated, as shown in Fig. 3. On the one hand, all the samples' ΔR_{DSON} decreases as the V_{GS} increases, on the other hand, the DT samples' ΔR_{DSON} consistently exceeds that of the AT samples. In fact, with the increase of the V_{GS}, the proportion of channel resistance begins to decrease, and the proportion of drift region resistance begins to increase. Furthermore, the drift region resistance is typically associated solely with the doping concentration and thickness. Based on these results, it can be inferred that the increase in the I_{DS} is attributable to the channel resistance variation. As a result, the following equations are used to calculate the main resistance component as

$$R_{DSON} \approx R_{CH1},\ V_{GS} = 6V, \tag{1}$$

$$R_{DSON} \approx R_{CH2} + R_D,\ V_{GS} = 12V, \tag{2}$$

$$R_{DSON} \approx R_D,\ V_{GS} = 18V. \tag{3}$$

Here, R_{CH1} is the channel resistance when the V_{GS} is 6V, R_{CH2} is the channel resistance when the V_{GS} is 12V, R_D is the drift region resistance. In Eq. 1, the channel just opens a little, leading to the channel resistance to be almost equal to the R_{DSON}. After selecting the same drain source voltage (V_{DS}), the values of the channel resistance have been calculated, i.e., R_{CH1}, for the DT and AT samples. In Eq. 2, the channel opens partially. Therefore, the R_{DSON} can be calculated as the sum of the channel resistance R_{CH2} and the R_D. In Eq. 3, the channel opens completely, making the R_D occupy a high proportion, which is almost equal to the R_{DSON}. After that, the values of the R_{CH1}, the R_{CH2}, and the R_D are successfully obtained and depicted in Fig. 4. It is easy to find that a remarkable decline occurs in the R_{CH1} and the R_{CH2} before and after the gamma ray irradiation. Specifically, the R_{CH1} and the R_{CH2} decrease 89% and 61% in the DT samples, while they decrease 57% and 21% in the AT samples. The R_D has rarely changed during the irradiation. These calculated results suggest that the main reason for the R_{DSON} degradation is the channel resistance.

In a word, the R_{DSON} degradation of the DT samples and the AT samples both are caused by the reduction of the channel resistance induced by the gamma ray irradiation. In particular, the channel resistance of the DT samples has an obvious decrease trend compared to that of the AT samples under the same irradiation with drain bias condition, which leads to the variations in their I_{DS}.

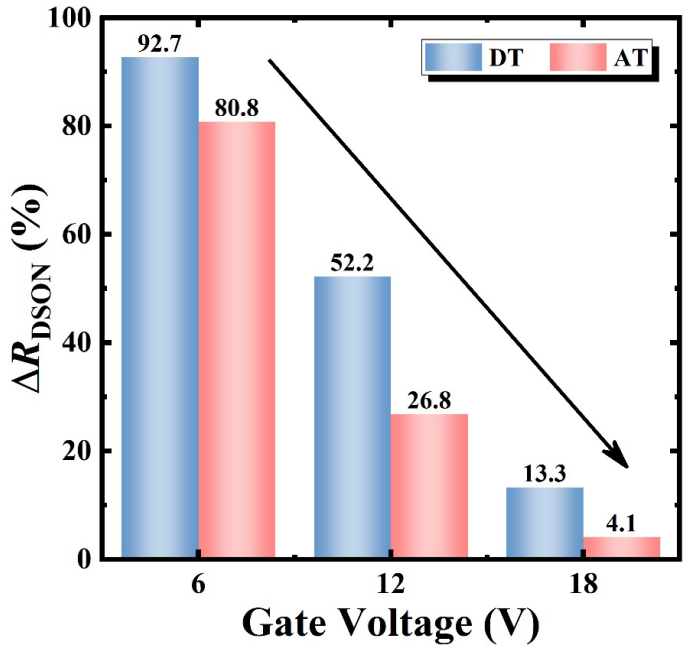

Fig. 3. ΔR_{DSON} results of the DT, and the AT samples before and after the TID irradiation.

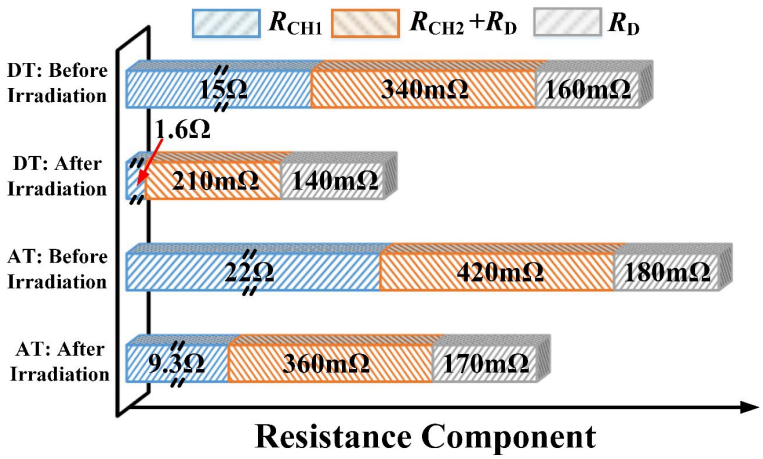

Fig. 4. Resistance Component of the DT, and the AT samples before and after the TID irradiation.

Subsequently, the V_{TH}, the I_{DSS}, and the I_{GSS} results are shown in Figs. 5-7. Fig. 5 illustrates that the TID effect damages the channel region of the DT and AT samples by introducing the positive charges into the gate oxide. In particular, the DT samples not only exhibit more heavily negative shifting than the AT samples, but also result in more current increase and the resistance decrease. In addition, the threshold voltage variations (ΔV_{TH}) results are listed in Table 3, the ΔV_{TH} of the DT samples is four times larger than that of the AT samples, indicating that the channel region of the DT samples is severely damaged. The V_{DS} also has no obvious impact on their ΔV_{TH}, which is the same as their variation in the I_{DS}.

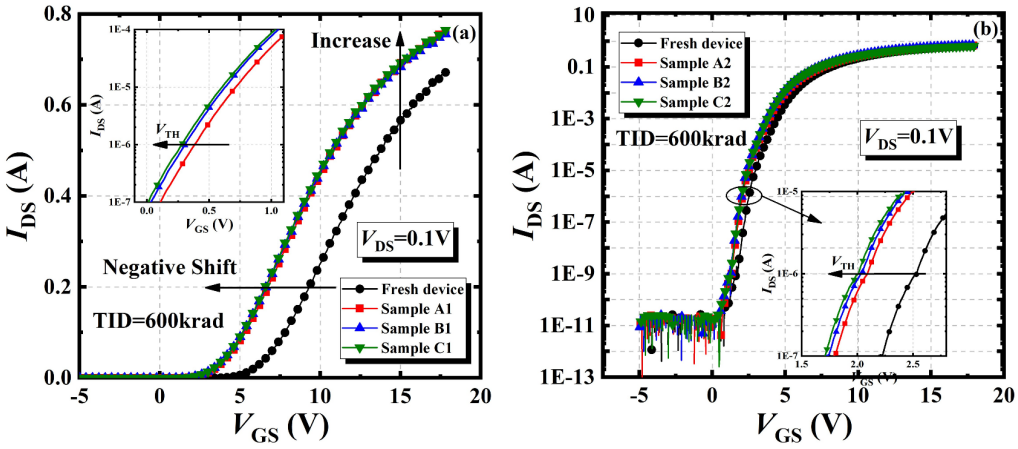

Fig. 5. Transfer characteristics of (a) the DT, and (b) the AT samples before and after the TID irradiation.

Table 3. Threshold Voltage Variation.

Type	ΔV_{TH}(V)		
	V_{DS}=600V	V_{DS}=800V	V_{DS}=1000V
DT	-1.87799	-1.99437	-2.0003
AT	-0.42214	-0.5229	-0.52483

Meanwhile, the I_{DSS} results are depicted in Fig. 6. Although the breakdown voltage of the DT and AT samples rarely shift after the TID irradiation, the I_{DSS} in DT samples has increased by four orders of magnitude in comparison with the fresh device. In contrast, the AT samples maintain a low I_{DSS} because of the minor fluctuations in the V_{TH}. Moreover, Fig. 7 shows that there is no obvious change

in the I_{GSS} for both of the DT and AT samples after the TID irradiation, because the I_{GSS} still remains at nA or pA level. The I_{GSS} of the DT and AT samples demonstrate insensitivity to the TID effect and the drain voltage bias. Notably, the AT samples invariably maintain an ultra-low I_{GSS} before and after the TID effect experiments, which can be attributed to the P-shield trench structure. This illustrates that the AT samples have better irradiation tolerance capability to the TID effect.

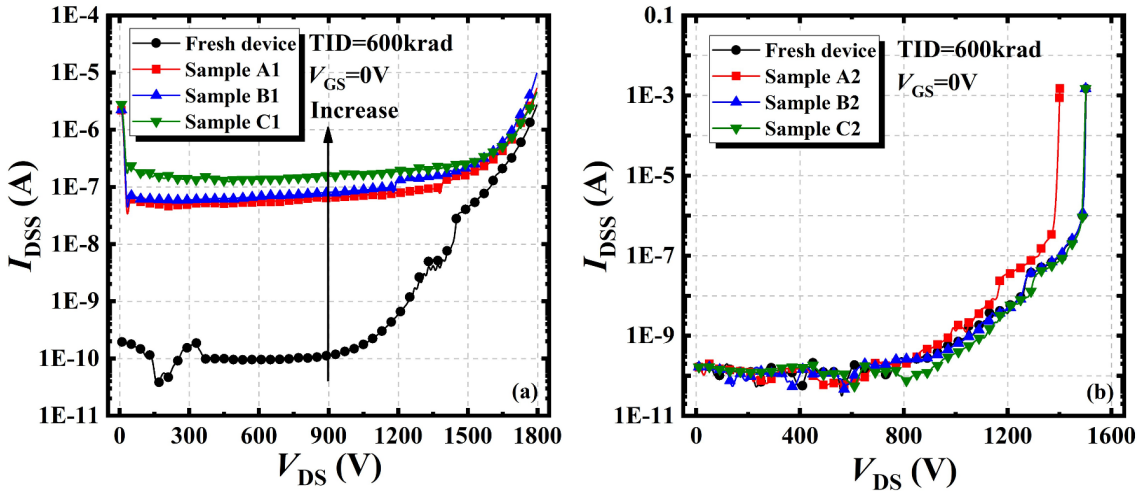

Fig. 6. Measured curves of I_{DSS}-V_{DS} of (a) the DT, and (b) the AT samples before and after the TID irradiation.

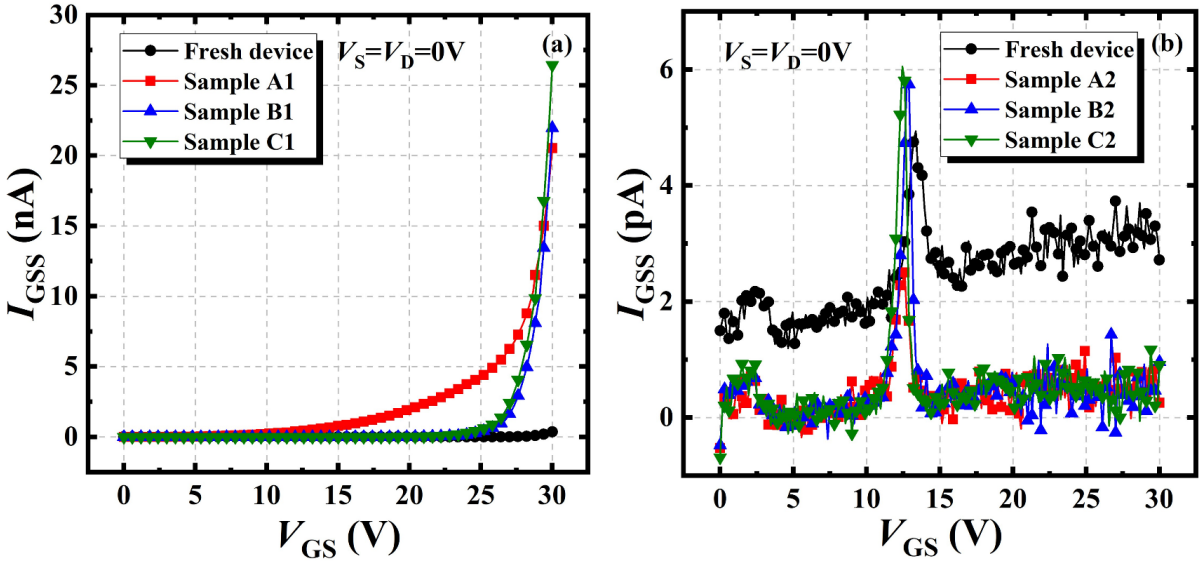

Fig. 7. Measured curves of I_{GSS}-V_{GS} of (a) the DT, and (b) the AT samples before and after the TID irradiation.

Finally, the TCAD simulations are performed to imitate the gamma ray irradiation process. The simulation results are presented in Figs. 8-10. It is observed that the TID effect introduces the holes into the gate oxide, producing the positive charges accumulation and thereby leading to the open of the channel, as shown in Fig. 8. In particular, Fig. 9 shows that the irradiation makes the current path change from the PN junction to the channel when the body diode (BD) of the DT samples is conducting in the forward direction, and the current density of the channel is much higher than that of the BD. Therefore, the DT sample's current density increases compared to the original one. Furthermore, the DT structure exhibits a more obvious increase trend in the total current density than the AT structure under the same irradiation and bias conditions based on Fig. 10. These simulations have good agreements with the measurements, proving the correctness of the mechanism.

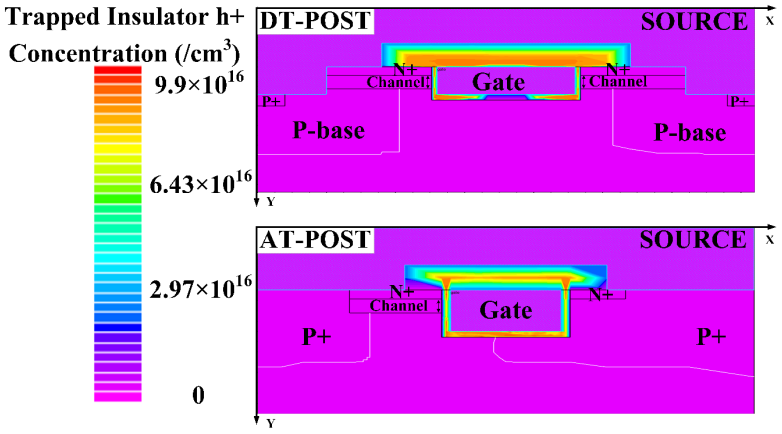

Fig. 8. Simulated trapped hole concentration of the DT, and the AT SiC MOSFET before and after the TID irradiation with drain voltage bias.

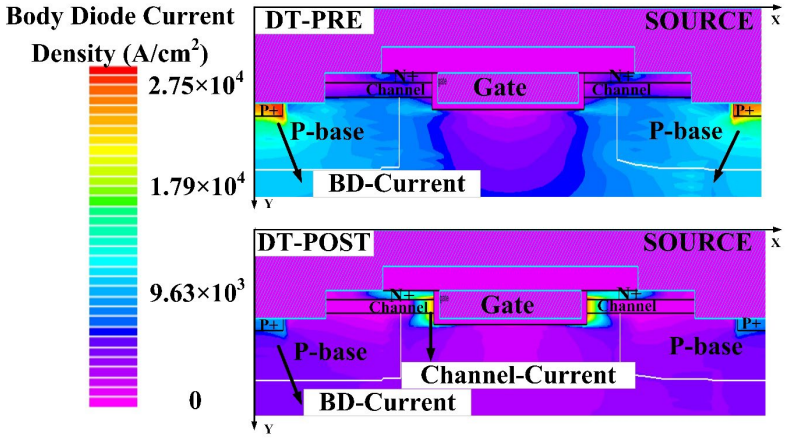

Fig. 9. Simulated body diode current density of the DT SiC MOSFET before and after the TID irradiation with drain voltage bias.

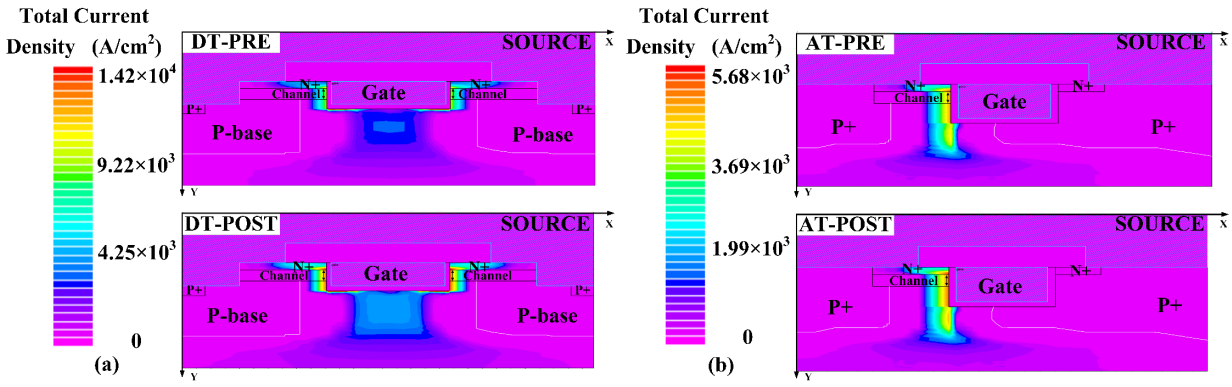

Fig. 10. Simulated total current density of (a) the DT, and (b) the AT SiC MOSFET before and after the TID irradiation with drain voltage bias.

Summary

The resistance degradation of the DT and the AT SiC MOSFETs exposed to the gamma ray irradiation with the high drain voltage bias is discussed in this work. The electrical characteristics results before and after the irradiation suggest that the reduction of their On-state resistance has a strong relation with their channel resistance. Especially, the degradation degree of DT sample on the R_{CH1} is more than 1.5 times that of AT sample, while the degradation degree on the R_{CH2} is almost 3 times that of AT samples based on the resistance component calculation, demonstrating that the channel resistance of the DT samples is more severely degraded. Besides, the ΔV_{TH} of the AT sample

before and after the irradiation is reduced by an order of magnitude compared to the DT samples and they are still maintaining ultra-low leakage current, proving that the P+ shield structure has better irradiation resistance to the TID effect. Ultimately, the simulation successfully imitates the irradiation and thereby verifies the degradation mechanism. Such an experiment has important guiding significance for the life assessment of the long-term operating devices in the space.

Acknowledgement

This work was supported in part by the National Natural Science Foundation of China under grants 62574042, 62434002, and U25B2059; in part by the Fundamental Research Funds for the Central Universities under grant 2242024RCB0028; in part by the Science and Technology Major Project of Jiangsu Province under grant BG2024001; in part by the Fund for Transformation of Scientific and Technological Achievements of Jiangsu Province under grant BA2023001; in part by the Natural Science Foundation of Jiangsu Province under grant BK20232027; and in part by the Distinguished Young Scientists Foundation of Jiangsu Province under grant BK20230025.

References

[1] L. Kong, S. Chen, N. Ren, M. Ji, Y. Li, H. Yan, Z. Liu, H. Xu, J. Cheng, X. Lin, X. Zhong, W. Chen, H. Huang, Y. Zhang and K. Sheng, "High-Performance 10-kV-Rated, 175-mΩ 4H-SiC MOSFETs With MeV JFET Implantation and Efficient Termination," in *IEEE Transactions on Electron Devices*, vol. 72, no. 8, pp. 4246-4253, Aug. 2025.

[2] S. Kim, Y. Park, D. Lee, J. Choi, M. Seo, B. Kwak, M. Kim and K. W. Ma, "Performance Evaluation of Sic Mosfet-Based Inverter for Individual Blade Control in Electrical Aircraft," *2025 IEEE/AIAA Transportation Electrification Conference and Electric Aircraft Technologies Symposium (ITEC+EATS)*, Anaheim, CA, USA, 2025, pp. 1-5, doi: 10.1109/ITEC63604.2025.11098042.

[3] R. Luo, Y. Duan, T. Luo, Y. Chang, W. Shi, X. Xu, J. Zhuang, G. Zhang and J. Fan, "Degradation Mechanism Analysis and Modeling of SiC MOSFETs Under 60Co Gamma Ray Total Ionizing Dose Irradiation," in *IEEE Transactions on Electron Devices*, vol. 72, no. 7, pp. 3437-3444, July 2025.

[4] C. Martinella *et al*., "Displacement Damage and Total Ionizing Dose Induced by 3-MeV Protons in SiC Vertical Power MOSFETs," in *IEEE Transactions on Nuclear Science*, vol. 72, no. 4, pp. 1259-1267, April 2025.

[5] H. G. de Medeiros, C. Martinella, M. Belanche, N. Für, P. Kumar, M. I. M. Martins, M. Nagel, S. Peracchi, R. Drury, Z. Pastuovic and U. Grossner, "Exploring the Relation Between SEEs Caused by Heavy-Ion Irradiation and Defects in SiC Devices," in *IEEE Transactions on Nuclear Science*, vol. 72, no. 8, pp. 2443-2451, Aug. 2025.

[6] J. Hu, X. Deng, Y. Wang, T. Xu, X. Li and B. Zhang, "An In-Depth Investigation of Gate Ringing Induced by Total Ionizing Dose in SiC MOSFETs," *2025 37th International Symposium on Power Semiconductor Devices and ICs (ISPSD)*, Kumamoto, Japan, 2025, pp. 577-580.

[7] T. Liu, R. Ma, Z. Wang, Q. Liu, H. Wang, J. Shen, J. Luo and S. Hu, "Comparative Investigation on TID-Induced Threshold Voltage Shift for 1200V Asymmetric Trench SiC MOSFET by Experiment and Simulation," *2025 6th International Conference on Radiation Effects of Electronic Devices (ICREED)*, Yangzhou, China, 2025, pp. 1-4.

[8] S. Liang, L. Shu, J. Wang, G. Deng and L. Wang, "Dynamic Degradation of Planar-Gate SiC MOSFETs After Total Ionizing Dose Radiation," in *IEEE Transactions on Electron Devices*, vol. 71, no. 7, pp. 4079-4086, July 2024.

[9] C. Peng, Z. Lei, Z. Zhang, Y. He, T. Ma and Y. Chen, “Bias and Temperature Dependence of Radiation-Induced Degradation for SiC MOSFETs,” in *IEEE Transactions on Nuclear Science*, vol. 71, no. 5, pp. 1186-1193, May 2024.

[10] H. Feng, X. Liang, X. Pu, S. Yang, J. Feng, Y. Wei, Y. Xiang, J. Sun, D. Zhang, Y. Li, Q. Yu, X. Yu and Q. Guo, “Special Degradation Effects of 60Co γ-Rays Irradiation on Electrical Parameters of SiC MOSFETs,” in *IEEE Transactions on Nuclear Science*, vol. 70, no. 9, pp. 2165-2174, Sept. 2023.

[11] A. Agarwal and B. J. Baliga, “Performance Enhancement of 2.3 kV 4H-SiC Planar-Gate MOSFETs Using Reduced Gate Oxide Thickness," in *IEEE Transactions on Electron Devices*, vol. 68, no. 10, pp. 5029-5033, Oct. 2021.

[12] Z. Dong, Y. Bai, C. Yang, C. Li, Y. Tang, J. Hao, X. Tian and X. Liu, “Impact of Post-Trench Process Treatment on Electron Scattering Mechanisms in 4H-SiC Trench MOSFETs,” in *IEEE Transactions on Electron Devices*, vol. 70, no. 4, pp. 1782-1788, April 2023.

[13] Z. Fu, Z. Shen, X. Tang, Y. Huang, J. Xu, K. Huang, Q. Zhang, Y. Chen, C. Xiao, K. Huang, S. Yue, Z. Wang and F. Zhang, “Comparative Study of TID Irradiation Effect on SiC Planar and Trench MOSFET,” *2024 21st China International Forum on Solid State Lighting & 2024 10th International Forum on Wide Bandgap Semiconductors (SSLCHINA: IFWS)*, Suzhou, China, 2024, pp. 123-129.

[14] R. Luo, Y. Duan, B. Sun, J. Q. Zhang, J. Fan and P. Liu, “Total Ionizing Effects on Static Characteristics of 1200V SiC MOSFET Power Devices with Planar and Trench Structures,” *2023 20th China International Forum on Solid State Lighting & 2023 9th International Forum on Wide Bandgap Semiconductors (SSLCHINA: IFWS)*, Xiamen, China, 2023, pp. 88-91, doi: 10.1109/SSLChinaIFWS60785.2023.10399707.